# Mutagenesis of E477 or K505 in the B′ Domain of Human Topoisomerase II$\beta$ Increases the Requirement for Magnesium Ions during Strand Passage

Katherine L. West,‡ Emma L. Meczes, Ronald Thorn, Rosalind M. Turnbull, Richard Marshall, and Caroline A. Austin*

*Department of Biochemistry and Genetics, The Medical School, The University of Newcastle Upon Tyne, Newcastle Upon Tyne NE2 4HH, U.K.*

*Received June 10, 1999; Revised Manuscript Received September 27, 1999*

ABSTRACT: A type II topoisomerase is essential for decatenating DNA replication products, and it accomplishes this task by passing one DNA duplex through a transient break in a second duplex. The B′ domain of topoisomerase II contains three highly conserved motifs, EGDSA, PL(R/K)GK(I/L/M)LNVR, and IMTD(Q/A)DXD. We have investigated these motifs in topoisomerase II$\beta$ by mutagenesis, and report that they play a critical role in establishing the DNA cleavage−religation equilibrium. In addition, the mutations E477Q (**E**GDSA) and K505E (PLRG**K**ILNVR) increase the optimal magnesium ion concentration for strand passage, without affecting the $Mg^{2+}$ dependence of ATP hydrolysis. It is likely that the binding affinity of the magnesium ion(s) specifically required for DNA cleavage has been reduced by these mutations. The crystal structure of yeast topo II indicates that residues E477 and K505 may help to position the three aspartate residues of the IMTD(Q/A)DXD motif for magnesium ion coordination, and we propose two possible locations for the magnesium ion binding site(s). These observations are consistent with a previous model in which the B′ domain is positioned such that these acidic residues lie next to the active site tyrosine residue. A magnesium ion bound by these aspartate residues could therefore mediate the DNA cleavage−religation reaction.

Topoisomerases are enzymes which relax the DNA supercoils that accumulate during transcription and replication; type II topoisomerases are also required for chromosome condensation and segregation (*1*−*4*). To carry out the strand passage reaction, topoisomerase II (topo II)[1] binds to two DNA helices termed the gate duplex and the transported duplex (*5*). The gate duplex is cleaved, generating 4 bp 5′-overhangs which are covalently linked to the enzyme via active site tyrosine residues (*6*−*8*). ATP binding, and possibly hydrolysis of one of the two ATP molecules (*9*, *10*), stimulates a conformational change which is concomitant with the passage of the transported helix through the enzyme-bridged break in the gate duplex (*11*, *12*). Hydrolysis of the remaining one or two ATP molecules is required for topo II to complete the catalytic cycle (*9*, *10*, *13*, *14*). In contrast, type I topoisomerases act by making a transient nick in one strand of the DNA double helix and allowing the other strand to rotate around it in an ATP-independent manner (*4*). Both type I and type II topoisomerases are targeted by anticancer drugs which stabilize the enzyme-cleaved DNA intermediate (*15*).

Topo II is comprised of four discrete functional domains: the N-terminal ATPase domain, the B′ domain, the breakage−reunion domain (A′ subfragment), and the C-terminal tail (*11*, *16*−*19*). X-ray crystallography has been used to determine the structure of the breakage−reunion domain of *Escherichia coli* DNA gyrase A (*20*), and also the structures of a 92 kDa fragment of *Saccharomyces cerevisiae* topo II in two different conformations, T2O (Figure 1) (*5*) and T2M (*21*). The three structures each represent a different stage in catalysis, with the gyrase A structure, termed T2C, representing the conformation which binds the gate duplex and initiates DNA cleavage. The active site tyrosine residue is located in the head region of the A′ subfragment, and in the DNA-open, T2O conformation, the A′ heads have been drawn apart to allow the transported helix to pass through (*5*). The recently published T2M structure (*21*) represents an intermediate stage between the DNA-closed conformation of T2C and the DNA-open conformation of T2O. The ATPase domains are thought to be located at the "top" of the yeast topo II structure shown in Figure 1A (*5*), where they may bind the transported DNA helix prior to strand passage (*22*, *23*).

The B′ domain is required for DNA cleavage by the breakage−reunion domain (*17*, *18*), and it contains three very highly conserved amino acid motifs which are characteristic of both prokaryotic and eukaryotic type II topoisomerases. Their sequences are EGDSA, PL(R/K)GK(I/L/M)LNVR, and IMTD(Q/A)DXD (Figure 2). Mutations in the first two motifs have been implicated in drug resistance in *E. coli* DNA gyrase, yeast topo II, and human topo II$\alpha$ (*24*−*28*). The central lobe of the B′ domain is comprised of a $\beta\alpha\beta\alpha\beta\alpha$ structure which resembles the "Rossmann" fold found in

* Corresponding author. Telephone: 44 191 222 8864. Fax: 44 191 222 7424. E-mail: Caroline.Austin@ncl.ac.uk.

‡ Current address: Laboratory of Molecular Carcinogenesis, Building 37, Room 3D-12, National Cancer Institute, National Institutes of Health, Bethesda, MD 20892.

[1] Abbreviations: m-AMSA, amsacrine; topo II, DNA topoisomerase II; topo I, DNA topoisomerase I.

10.1021/bi991328b CCC: $19.00 
Published on Web 01/19/2000

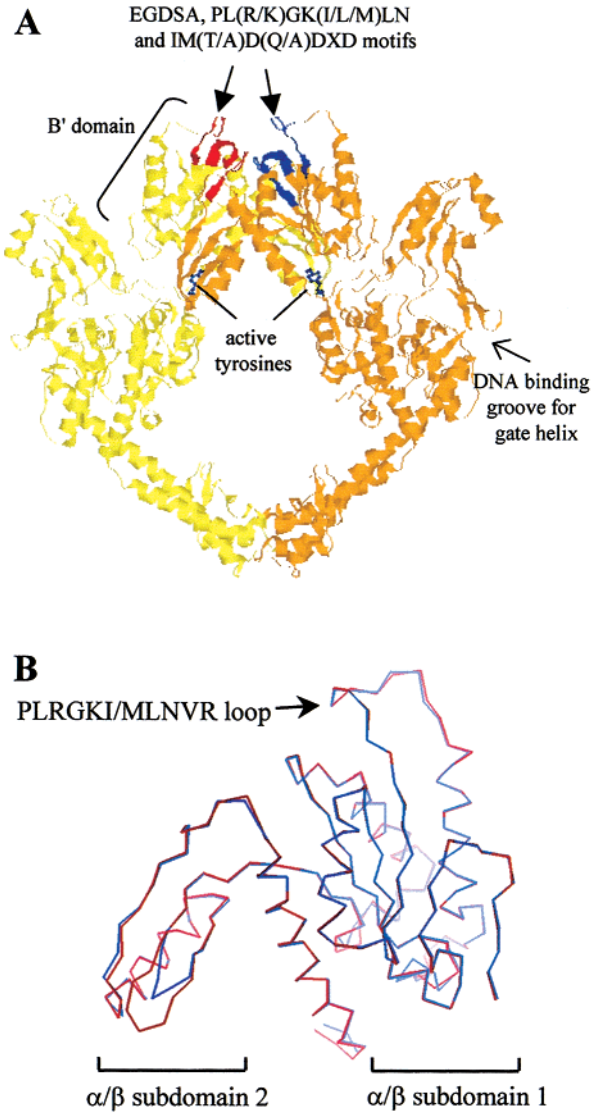


FIGURE 1: (A) Crystal structure of a 92 kDa fragment of *S. cerevisiae* topo II in the T2O conformation (**5**). The EGDSA, PL(R/K)GK(I/L/M)LNVR, and IMTD(Q/A)DXD motifs are shown in red on the yellow monomer and in blue on the orange monomer. The active site tyrosine residues are shown in blue. (B) Modeling the structure of the B′ subfragment of topoisomerase II$\beta$. Residues 447−658 of human topo II$\beta$ (blue) were modeled onto residues 420−632 of *S. cerevisiae* topo II (red) using the computer program Modeller, based on the alignment of Caron and Wang (*31*). The two structures are superimposed, and the only region of significant divergence is in the loop between two $\beta$-sheets in $\alpha/\beta$ subdomain 2.

nucleotide binding proteins (*5*, *29*). The three conserved motifs are located on different loops between the secondary structure elements of this fold (Figure 1), and hydrogen bonds are predicted to occur between the motifs (*5*).

Insights into the roles of some of these conserved residues may come from comparisons with the type 1A topoisomerases. The secondary structure of domain 1 of *E. coli* topoisomerase I (topo I) is similar to that of the topo II B′ domain, and it also adopts a Rossmann fold conformation (*30*). The glutamate residue at the start of the topo II EGDSA motif is conserved in type IA enzymes, as are the three aspartate residues of the IMTD(Q/A)DXD motif (*29*, *31*). The X-ray crystal structure of *E. coli* topo I reveals that the arrangement of these three conserved aspartate residues near the active site tyrosine residue resembles that of three acidic residues in the active site of the Klenow fragment of *E. coli* DNA polymerase (*30*, *32*). In the latter enzyme, these residues are required for binding two magnesium ions, one of which facilitates the formation of the hydroxyl ion that attacks the DNA backbone (*32*). Indeed, in nearly all DNA polymerases, the catalytic magnesium ions are coordinated by three conserved acidic residues (*33*−*37*). It is possible, therefore, that the conserved acidic residues in topo I also play a role in magnesium ion coordination. In yeast topo II, the IMTD(Q/A)DXD motif is approximately 40 Å from the active site tyrosine residue in the DNA-open T2O structure (*5*). However, the B′ domain is rotated by 170° in the T2M structure so that this motif is only 20 Å from the active site (*21*). Molecular modeling has been employed to predict the orientation of the B′ domain in the DNA-closed conformation (*29*), based on the gyrase A T2C structure (*20*) and the orientation of domain 1 from *E. coli* topo I (*30*). This modeling indicated that the B′ domain may be further rotated in the DNA-closed conformation, bringing the IMTD(Q/A)DXD motif into the vicinity of the active site.

Higher vertebrates have two closely related topo II isoforms, α and $\beta$, both of which catalyze ATP-dependent strand passage in vitro and in vivo, and both are targets for anticancer agents (*38*, and references therein). In human tissues, the α isoform is found predominantly in proliferating cells, whereas the $\beta$ isoform is found in all tissues, including those which are fully differentiated (*38*). Topo IIα appears to be required for chromosome segregation, but the precise function of the $\beta$ isoform has yet to be elucidated. Computer modeling reveals that the structure of the B′ domain in human topo II$\beta$ is very similar to that of yeast topo II (Figure 1B). We have adopted a mutagenic approach to investigating the roles of the EGDSA, PL(R/K)GK(I/L/M)LNVR, and IMTD(Q/A)DXD motifs in catalysis by human topo II$\beta$. Proteins with mutations at highly conserved charged or polar residues within these motifs were assayed in vivo by complementation assays, and in vitro for DNA strand passage, ATP hydrolysis, DNA binding, and DNA cleavage activities. All of the mutations significantly reduced the DNA cleavage activity of topo II$\beta$, and in addition, two mutations increased the optimal magnesium ion concentration required for strand passage activity. With reference to the X-ray crystal structures of yeast topoisomerase II and *E. coli* DNA gyrase A (*5*, *20*, *21*), we present a model for the magnesium ion binding site, and discuss the role of the B′ domain in the catalytic cycle of topo II$\beta$.

## EXPERIMENTAL PROCEDURES

*Mutagenesis of Topoisomerase II$\beta$.* Mutagenesis was carried out using the restriction site elimination method (Stratagene). Mutagenesis was initially carried out on plasmid YEphTOP2$\beta$, which is the yeast expression plasmid for recombinant human topo II$\beta$S165R (*19*). The S165R mutation was reversed to give the wild-type (wt) sequence, and the new plasmid was named YEphTOP2$\beta$-KLM (*39*). In this recombinant protein, the first 45 amino acid residues of topo II$\beta$ are replaced with the first five residues of *S. cerevisiae* topo II (*19*). For simplicity, the recombinant protein produced from plasmid YEphTOP2$\beta$-KLM is termed wt topo II$\beta$ hereafter. Further mutations were created by mutagenesis of plasmid YEphTOP2$\beta$-KLM.

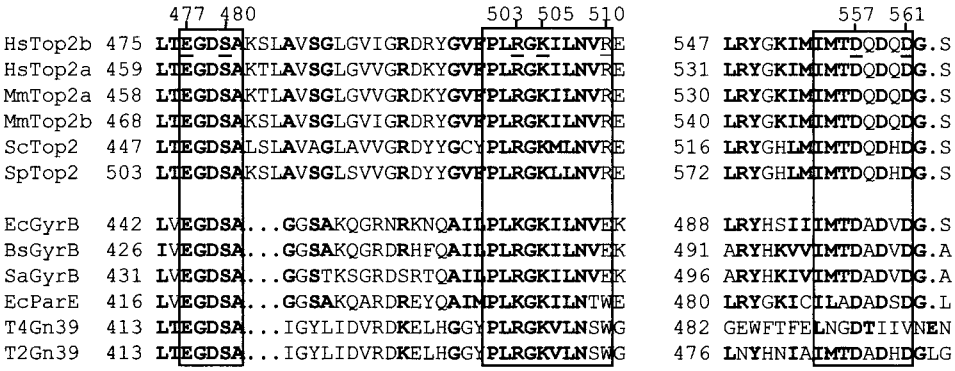


FIGURE 2: Alignment of the EGDSA, PL(R/K)GK(I/L/M)LNVR, and IMTD(Q/A)DXD regions from eukaryotic, prokaryotic, and bacteriophage type II topoisomerases (*31*). Conserved residues are shown in bold. The conserved motifs are enclosed by boxes.

Mutagenic oligonucleotides are as follows (substituted nucleotides are underlined): selection primer for converting an *Eco*RV site to a *Sac*II site, CCTCCATGGAAAAATCAGTCAAGAGCTCCACATGTG; and selection primer for converting the *Sac*II site back to the *Eco*RV site, CCTCCATGGAAAAATCAGTCAAGATATCCACATGTG; E477Q, CACTGATATTAACCCAGGGAGACTC; S480A, GAGGGAGACGCTGCCAAATCACTGG; R503E, GGAGTTTTTCCACTCA/GA/CGGGCAAAATTC; K505E, GGGGCGA/CAATTCTTAATGTACGG; R510Q, GGGGCAAAATTCTTAATGTAA/CAGGAAGCTTCTC; D557N, GATTATGACCAATCAGGATCAAG; and D561N, CCGATCAGGATCAAAATGGTTCTCAC.

Mutant proteins $\beta$S480A, $\beta$R503E, $\beta$R510Q, $\beta$D557N, and $\beta$D561N were overproduced in *S. cerevisiae* strain JEL1 ($\alpha$ *leu2 trp1 ura3-52 prb1-1122 pep4-3* Δ*his3::PGAL 10-GAL4*) (*40*). Wt topo II$\beta$ and the mutant proteins $\beta$E477Q and $\beta$K505E were overproduced in strain JEL1 Δ*top1*, kindly provided by R. Hanai (Department of Chemistry, Rikkyo University, Tokyo, Japan). Wt and mutant topo II$\beta$ derivatives were purified as described previously (*19*).

*Complementation Analysis.* The viability of *S. cerevisiae* strain JN394*t2-4* (*41*) transformed with plasmids expressing wt or mutant topo II$\beta$ was tested at 25 and 35 °C on rich medium containing glucose, raffinose, or galactose as described previously (*39*).

*Strand Passage Activity Assays.* Decatenation and relaxation assays were carried out in relaxation buffer [50 mM Tris-HCl (pH 7.5), 0.5 mM EDTA, 1 mM DTT, 50 mM KCl, and 30 $\mu$g/mL BSA] with 1 $\mu$g of supercoiled plasmid DNA or 400 ng of kinetoplast DNA, 1 mM ATP, and 10 mM $MgCl_2$ as described previously (*19*). Agarose gels were photographed with a Bio-Rad geldoc 1000 imager and analyzed using Tina version 2.08e software. Preparations of the mutant protein $\beta$S480A, $\beta$R503E, and $\beta$R510Q contained some topo I activity, as they were overproduced in a yeast strain containing topo I. The relaxation of supercoiled plasmid DNA by topo II is an ATP-dependent process, whereas relaxation by topo I is ATP-independent. Therefore, relaxation assays were performed at increasing protein concentrations both in the presence and in the absence of ATP, and the difference in relaxation between the two data sets was taken as topo II relaxation activity. Mutants $\beta$E477Q and $\beta$K505E did not contain topo I activity, and thus, the relaxation activity was assessed by the protein concentration required to relax 50% of the input supercoiled DNA.

*Assay for ATP Hydrolysis Activity.* ATP hydrolysis was assayed by a coupled enzyme assay (*40*), which links ATP hydrolysis to NADH oxidation. Topo II (50 nM) was incubated with 1 mM ATP, 20 $\mu$g/mL pBluescript-derived plasmid, 2 mM phosphoenolpyruvate (PEP), 0.1 mM NADH, 5 units of lactate dehydrogenase, and 2.5 units of pyruvate kinase in relaxation buffer at 30 °C. The rate of NADH oxidation was measured by the decrease in absorbance at 340 nm, and is directly proportional to the rate of ATP hydrolysis. All components except topo II and ATP were in excess, as the doubling of the concentration of any component did not increase the rate of NADH oxidation. No NADH oxidation was observed in the absence of ATP.

*Gel Retardation Analysis.* The 40 bp linear DNA substrate was made using oligos C and D, whereas the four-way junction was made with oligos O1−4. Topo II$\beta$ cleaves the linear substrate between the nucleotides which are underlined on oligos C and D: C, CGCAATCTGACAATGCGCTCATCGTCATCCTCGGCAC; D, CGCGTGCCGAGGATGACGATGAGCGCATTGTCAGATT; O1, CTGGACGCAATCTGACAATGCGCTCATCGTCATCCTCGGCACGC; O2, CGGCGCGTGCCGAGGATGACGATGAGATAGGCGTTAACGCGG; O3, TAGGCCGCGTTAACGCCTATTTGCCCGGGAGTACCGGCAT; and O4, AGGAATGCCGGTACTCCCGGGCAACGCATTGTCAGATTGCGT.

The oligos were end-labeled by T4 PNK in the presence of [$\gamma$-$^{32}$P]ATP and annealed, and then the linear duplex or four-way junction was gel purified as described previously (*42*). Binding reactions were carried out for 45 min on ice in 20 $\mu$L of GR buffer {gel retardation assay buffer [50 mM Tris-HCl (pH 7.5), 0.5 mM EDTA, 1 mM DTT, 50 mM KCl, 1% Triton X-100, and 5% glycerol]} with 30 $\mu$g/mL BSA (linear substrate) or 1 mg/mL BSA (four-way junction substrate). Samples were electrophoresed at 4 °C on 6% 37.5:1 (linear substrate) or on 5% 80:1 (four-way junction substrate) polyacrylamide gels with 50 mM Tris-glycine (pH 9.2) (*43*) as the running buffer (*42*).

*Cleavage of the Linear DNA Substrate.* Cleavage reaction mixtures contained 600 ng of topo II$\beta$-derived protein and the 40 bp linear substrate which had been labeled at both 5′-ends. Reactions were carried out in GR buffer with 10 mM $MgCl_2$ or $CaCl_2$ in the presence or absence of 10 $\mu$g/mL *m*-AMSA, and processed as described previously (*19*).

## RESULTS

*In Vivo Complementation Analysis of Topo II$\beta$ Mutants.* The B′ domain of human topo II$\beta$ contains three adjacent,

Table 1: Growth of JN394*t2-4* Transformed with Plasmids Bearing Topo II$\beta$ Mutants on Different Media at 35 °C[a]

| | YPA and glucose | YPA and raffinose | YPA and galactose |
|---|---|---|---|
| yeast topo II | +++ | +++ | − |
| wt topo II$\beta$ | +++ | ++ | − |
| E477Q | − | − | − |
| S480A | ± | − | − |
| R503E | − | − | − |
| R505E | − | − | − |
| R510Q | + | + | − |

[a] Liquid cultures of each strain were grown in glucose-containing minimal medium at 25 °C to an optical density of 1.0 at 600 nm before being serially diluted in a microtiter tray. The diluted cultures were then imprinted onto agar plates containing the listed medium and incubated at 25, 30, and 35 °C. The results of the 35 °C incubations only are shown here. No growth is indicated by a minus sign and poor to proliferous growth by ±, +, ++, and +++ symbols. The extent of growth was determined with respect to growth at the permissive and semipermissive temperatures and by the degrees of growth at each of the serial dilutions.

highly conserved amino acid motifs: EGDSA (residues 447−481), PL(R/K)GK(I/L/M)LNVR (residues 501−510), and IMTD(Q/A)DXD (residues 554−561) (Figure 2). A mutagenic approach was taken to investigate the importance of these motifs in the catalytic cycle of topo II. The mutations D557N and D561N within the IMT**D**QDQ**D** motif were created to address the question of whether these conserved aspartate residues participate in metal ion coordination. Several other highly conserved charged or polar residues within these motifs were also mutated to investigate their roles in catalysis: E477Q, S480A (**E**GD**S**A), R503E, K505E, and R510Q (PL**R**G**K**ILNV**R**) (Figure 2).

Complementation assays were used to determine whether the mutant proteins retained sufficient activity to carry out the essential roles of topo II in vivo. Plasmids expressing wild-type or mutant topo II$\beta$ derivatives were transformed into an *S. cerevisiae* strain in which the chromosomal gene encoding topo II carries a temperature sensitive mutation, *top2-4* (*41*). This strain cannot grow at the nonpermissive temperature of 35 °C due to the absence of topo II activity, but it can be rescued by transformation with a plasmid expressing active topo II. Expression of the plasmid-borne topo II was controlled by a galactose-inducible promoter. A range of dilutions for each mutant was spotted onto agar plates containing glucose, raffinose, or galactose, and the extent of colony growth at 25 and 35 °C was scored (Table 1). As previously shown, wt topo II$\beta$ could complement *ts* topo II at the nonpermissive temperature (*39*). In contrast, mutants $\beta$E477Q, $\beta$R503E, $\beta$K505E, $\beta$D557N, and $\beta$D561N were not able to complement *ts* topo II under the conditions that were studied. $\beta$S480A and $\beta$R510Q complemented each other to a limited extent, conferring slow growth on the yeast at 35 °C (Table 1). For the complementing plasmids, growth was strongest in the presence of glucose, when only a small amount of topo II is transcribed from the GAL1 promoter. Growth was abolished when wt topo II$\beta$, $\beta$S480A, or $\beta$R510Q was overexpressed in the presence of galactose, in accordance with previous observations that overexpression of topo II is toxic to yeast cells (*8*). These results show that each of the mutations (E477Q, R503E, K505E, D557N, and D561N) reduces the activity of topo II$\beta$ such that it can no longer perform its essential role in vivo, whereas some in vivo activity is retained in mutants S480A and R510Q.

*Strand Passage Activity of Purified Wild-Type and Mutant Enzymes.* To further characterize the mutant topo II$\beta$ enzymes, the plasmid-borne genes were overexpressed by galactose induction and the mutant enzymes purified. Although $\beta$D557N and $\beta$D561N were overexpressed to high levels, the proteins were very unstable and were rapidly degraded during subsequent purification steps. No strand passage activity was detected for either of these mutant proteins prior to degradation. These data indicate that these mutations have induced an altered conformation that is more susceptible to proteolysis, and further characterization of these mutants was not attempted.

Purified wt topo II$\beta$ and the other mutants were assayed for decatenation and relaxation activity to characterize the full catalytic cycle. Decatenation of kinetoplast DNA (kDNA) by topo II results in the release of individual minicircles from the kDNA network, a reaction which topo I cannot perform. Figure 3a−e shows that decatenation activity increases with increasing concentrations of wt topo II$\beta$, $\beta$S480A, $\beta$R503E, $\beta$R505E, and $\beta$R510Q. Specific activities were compared by calculating the concentration of enzyme required to decatenate 50% of the substrate (Figure 3f,g). The mutants with the lowest decatenation activities were $\beta$K505E (Figure 3d,g,i) and $\beta$E477Q (Figure 3i), which only had 7−8% of the wt topo II$\beta$ activity. The decatenation activity of $\beta$R503E was 35% of that exhibited by wt topo II$\beta$, whereas $\beta$S480A and $\beta$R510Q were more active, exhibiting 59 and 74% of the wt topo II$\beta$ activity, respectively (Figure 3i).

The abilities of the mutants to relax supercoiled plasmid DNA were also assayed (Figure 3i). Again, $\beta$E477Q and $\beta$K505E had the lowest activity, with only 2 and 6% of the wt topo II$\beta$ relaxation activity, respectively (Figure 3h). Mutants $\beta$S480A, $\beta$R503E, and $\beta$R510Q all had similar levels of activity in this assay (49−68% of the wt topo II$\beta$ activity). Figure 3i also shows that both decatenation and relaxation assays yield comparable estimates for the relative strand passage activities of the mutant proteins.

It is possible that the inability of some of the mutants to complement *ts* topo II arises from a temperature sensitive phenotype. However, decatenation assays performed at 4, 23, and 37 °C revealed that none of the mutant proteins had significant temperature sensitivity (data not shown). It can be concluded that mutations R503E, S480A, and R510Q reduced the strand passage activity of topo II$\beta$ by 25−65%, whereas mutations E477Q and K505E reduced strand passage activity by more than 90%.

*Effect of Magnesium Ion Concentration on Decatenation Activity.* Topo II requires magnesium ions for ATP binding and hydrolysis (*45*). In addition, either magnesium or calcium ions are required for DNA cleavage (*45*). Therefore, the magnesium dependence of decatenation by each mutant was examined. Wt topo II$\beta$, $\beta$S480A, $\beta$R503E, and $\beta$R510Q exhibited maximal activity between 3 and 20 mM $Mg^{2+}$ (Figure 4a). In contrast, mutants $\beta$E477Q and $\beta$K505E exhibited a narrower optimum of 15−20 mM $Mg^{2+}$ (Figure 4c,d).

To determine whether the narrower $Mg^{2+}$ optima for $\beta$E477Q and $\beta$K505E resulted from an increase in the affinity for $Mg^{2+}$, the experiments were repeated using equal concentrations of each protein (Figure 4e). The maximal decatenation activities of $\beta$E477Q and $\beta$K505E were 10%

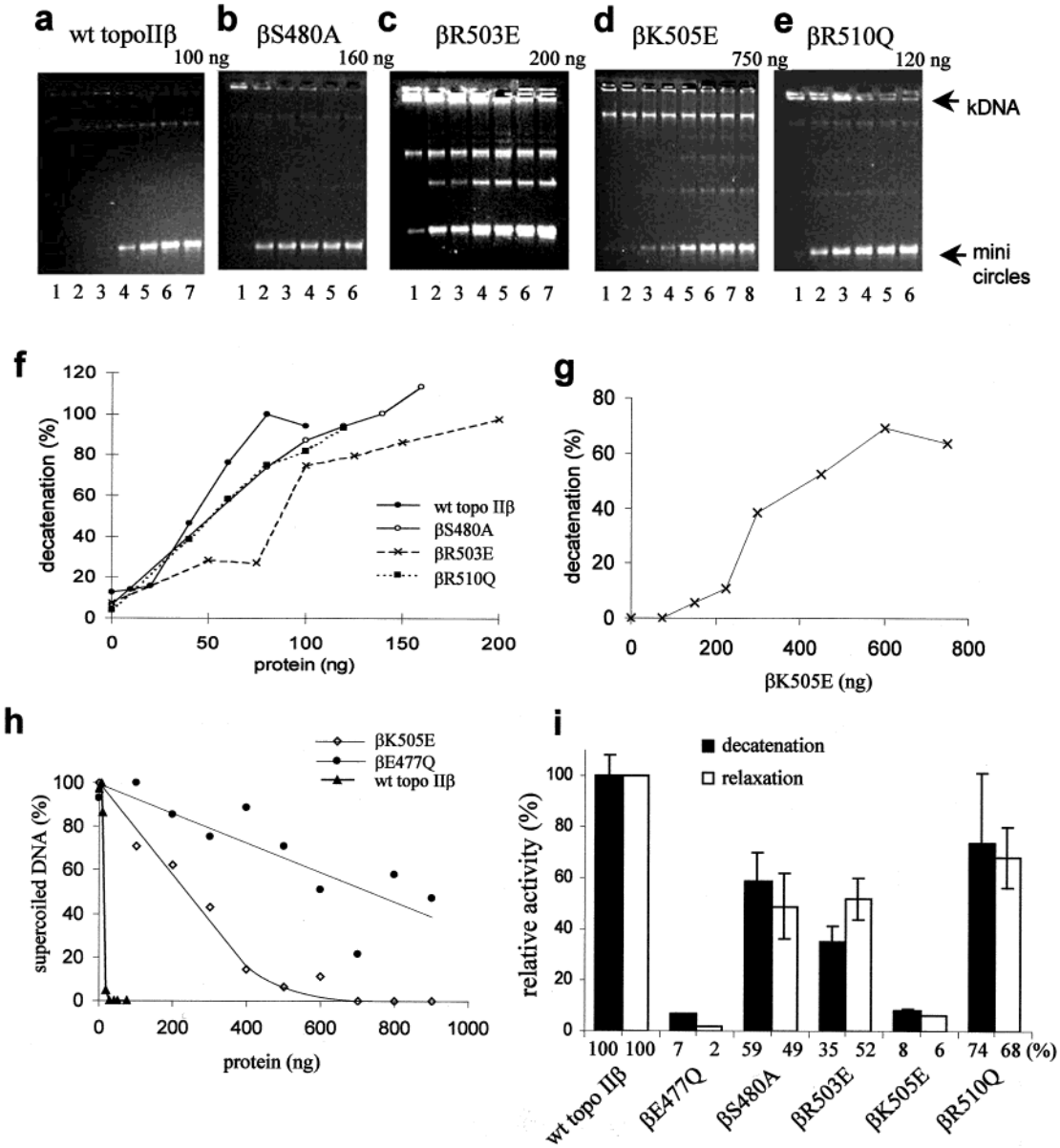


FIGURE 3: Strand passage activity of wt and mutant topo II$\beta$ derivatives. Decatenation of kinetoplast DNA by wt topo II$\beta$, $\beta$S480A, $\beta$R503E, $\beta$K505E, and $\beta$R510Q is shown in parts a−e, respectively. (a) Wt topo II$\beta$ was present in amounts of 0, 10, 20, 40, 60, 80, and 100 ng in lanes 1−7, respectively. (b) $\beta$S480A was present in amounts of 0, 80, 100, 120, 140, and 160 ng in lanes 1−6, respectively. (c) $\beta$R503E was present in amounts of 0, 50, 75, 100, 125, 150, and 200 ng in lanes 1−7, respectively. (d) $\beta$K505E was present in amounts of 0, 75, 150, 225, 300, 450, 600, and 750 ng in lanes 1−8, respectively. (e) $\beta$R510Q was present in amounts of 0, 40, 60, 80, 100, and 120 ng in lanes 1−6, respectively. Decatenation was quantified as a percentage of a 100% decatenation control, and is plotted against protein concentration in graphs f and g. (f) (●) wt topo II$\beta$, (○) $\beta$S480A, (×) $\beta$R503E, and (■) $\beta$R510Q. (g) $\beta$K505E. The amount of protein required for 50% decatenation was measured off each curve in parts f and g, and means were calculated from at least two experiments for each mutant. The inverse of each mean, expressed as a percentage of that for wt topo II$\beta$, is plotted as decatenation activity in part i; error bars represent one standard deviation ($SD^{n-1}$) from the mean. (h) Relaxation of supercoiled DNA by increasing concentrations of wt topo II$\beta$ (▲), $\beta$E477Q (●), and $\beta$K505E (◇). Relative relaxation activity was calculated by determining the protein concentration required to relax 50% of the supercoiled DNA. The reciprocal of this concentration, expressed relative to that for wt topo II$\beta$, is plotted in part i. (i) Relative decatenation (black bars) and relaxation (white bars) activities for wt topo II$\beta$ and its mutants. The numerical values are shown beneath each column. The relaxation activities of wt topo II$\beta$, $\beta$S480A, $\beta$R503E, and $\beta$R501Q were assayed by incubating increasing amounts of protein with supercoiled plasmid DNA in the presence or absence of 1 mM ATP (not shown). Relaxation activity due to topo II was calculated by subtracting activity in the absence of ATP (topo I activity) from activity in the presence of ATP. Topo II relaxation activity was plotted against protein level, and the initial gradient of the slope was taken as the specific relaxation activity of the mutant protein. Means were calculated from at least two experiments, and error bars represent one standard deviation ($SD^{n-1}$) from the mean.

(±5) of that for wt topo II$\beta$, and so a 10-fold shorter reaction time was used for wt topo II$\beta$ than for $\beta$E477Q and $\beta$K505E. From these experiments, the apparent affinity (apparent $K_M$) of wt topo II$\beta$ for $Mg^{2+}$ ions was calculated to be 2.6 mM, whereas the affinities of $\beta$E477Q and $\beta$K505E were both 9.7 mM, an increase of 3.7-fold.

To rule out the possibility that these $\beta$E477Q and $\beta$K505E simply have maximal activity at higher salt concentrations than wt topo II$\beta$, relaxation assays were carried out at a range of KCl concentrations. All three proteins had a very similar dependence on salt concentration between 50 and 200 mM KCl (data not shown), indicating that the requirement for

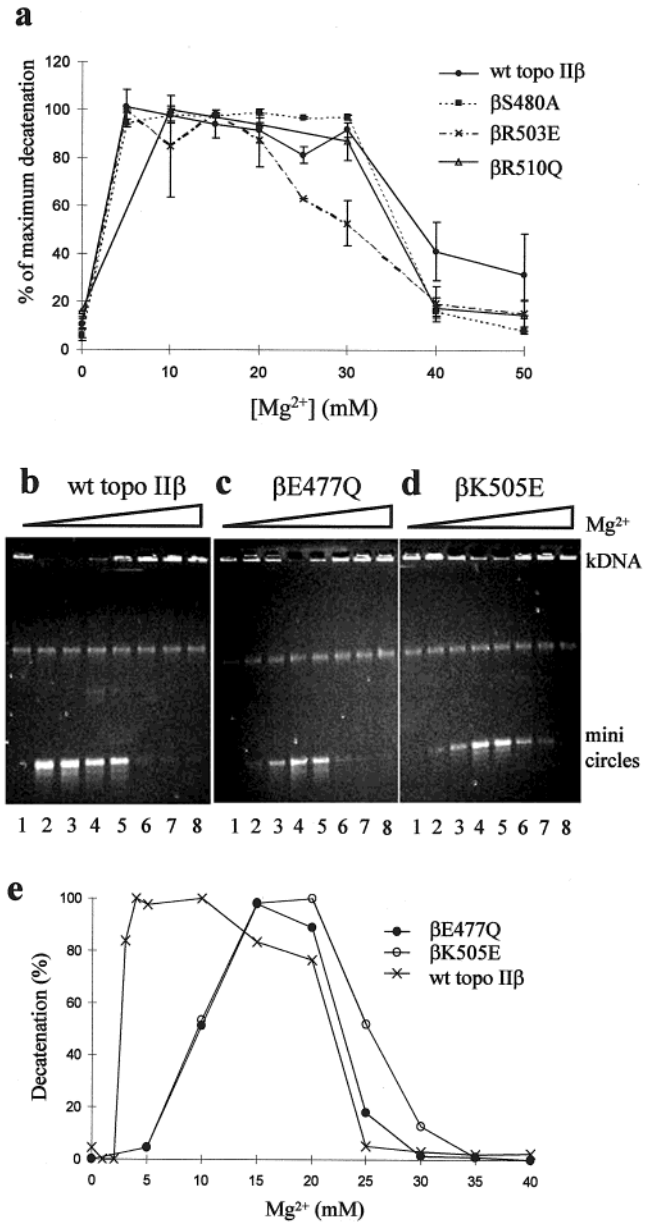


FIGURE 4: Effect of $Mg^{2+}$ concentration on decatenation by wt and mutant topo II$\beta$ derivatives. (a) The decatenation activity of wt topo II$\beta$ (●), $\beta$S480A (■), $\beta$R503E (×), and $\beta$R510Q (△) was assayed at a range of $Mg^{2+}$ concentrations. The concentration of each protein was chosen such that no more than 80% of the substrate would be decatenated within the 30 min reaction time. Means and standard deviations ($SD^{n-1}$) were derived from three independent experiments. (b−d) Decatenation by (b) 15 ng of wt topo II$\beta$, (c) 500 ng of $\beta$E477Q, and (d) 500 ng of $\beta$K505E was carried out at 0, 5, 10, 15, 20, 25, 30, and 40 mM $Mg^{2+}$ in lanes 1−8, respectively. (e) Decatenation by 500 ng of wt topo II$\beta$ (×), $\beta$E477Q (●), and $\beta$K505E (○) was carried out at 37 °C for 3 min (wt topo II$\beta$) or 30 min ($\beta$E477Q and $\beta$K505E) to give equivalent levels of decatenation activity for each protein. Under these conditions, no more than 70% of the substrate was decatenated during the reactions, and there was a linear relationship between the percentage of decatenation and reaction time. The level of decatenation was quantified as a percentage of the maximum for each protein, and is plotted against $Mg^{2+}$ concentration (millimolar). EDTA was present at a concentration of less than 0.15 mM. The apparent $K_M$ was calculated from the graph by determining the magnesium ion concentration required for half-maximal activity.

increased magnesium does not arise from an altered response to ionic strength. The specific requirement for an increased $Mg^{2+}$ concentration strongly suggests that the mutations

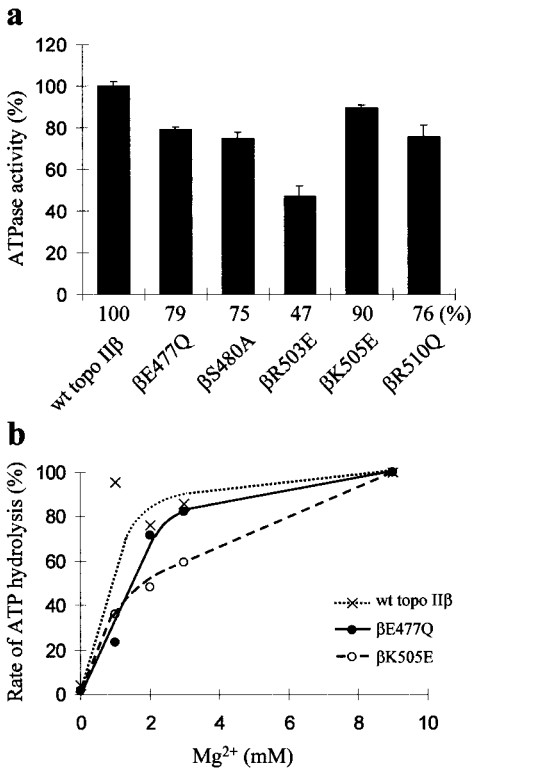


FIGURE 5: ATP hydrolysis by wt and mutant topoisomerase II$\beta$ derivatives. (a) The ATP hydrolysis activities of wt and mutant topo II$\beta$ derivatives (50 nM) were assayed in the presence of 10 mM $MgCl_2$. The mean for wt topo II$\beta$ was set to 100%, and error bars represent one standard deviation from the mean ($SD^{n-1}$). (b) The ATP hydrolysis activities of 350 nM wt topo II$\beta$ (×), $\beta$E477Q (●), and $\beta$K505E (○) were assayed at increasing $MgCl_2$ concentrations. The maximum rate for each protein was set to 100%. The $Mg^{2+}$ concentrations shown in this figure have been corrected for the presence of 1 mM EDTA in the reaction so as to facilitate comparison with the decatenation data.

E477Q and K505E have reduced the affinity of topo II$\beta$ for magnesium ions by disrupting one or more cation binding sites.

*ATP Hydrolysis Activity.* It is possible that the increased requirement for $Mg^{2+}$ demonstrated by $\beta$E447Q and $\beta$K505E is related to changes in the interaction of Mg-ATP with the ATPase domain. To address this question, and to determine whether the reduced strand passage activity observed for the other mutants is derived from reduced ATPase activity, the rates of ATP hydrolysis for each protein were assayed. At saturating ATP concentrations, ATP hydrolysis is uncoupled from strand passage, and thus, the rate of ATP hydrolysis can be assayed independently (*40*). In the presence of DNA, the rate of ATP hydrolysis increased linearly with the amount of wt topo II$\beta$ present (K. L. West et al., unpublished data). As shown in Figure 5a, mutants $\beta$S480A, $\beta$E477Q, $\beta$K505E, and $\beta$R510Q exhibited ATP hydrolysis activities similar to that of wt topo II$\beta$ in the presence of DNA (all greater than 75%), whereas mutant $\beta$R503E had only 47% ATPase activity. In the absence of DNA, the variation of ATPase activity with protein levels was too low to measure reproducibly.

The rates of ATP hydrolysis by $\beta$E477Q and $\beta$K505E were assayed at a range of $Mg^{2+}$ concentrations, to determine whether the altered $Mg^{2+}$ dependence observed for decatenation by these mutants was also observed for ATP

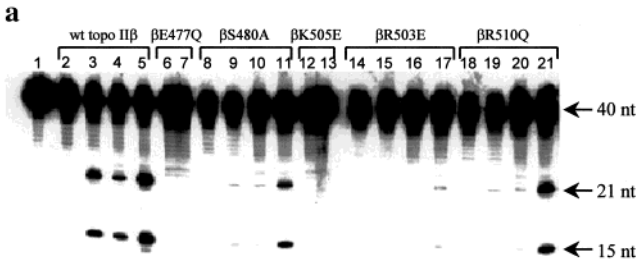


b

| | $Mg^{2+}$, m-AMSA | $Ca^{2+}$ | $Ca^{2+}$, m-AMSA |
|---|---|---|---|
| wt topo IIβ | 100 | 51 +/- 18 | 257 +/- 61 |
| βS480A | 19 +/- 17 | 10 +/- 5 | 59 +/- 8 |
| βR503E | 0.5 +/- 0.6 | 2.1 +/- 1.5 | 22 +/- 1 |
| βR510Q | 13 +/- 10 | 12 +/- 6 | 110 +/- 27 |

FIGURE 6: Cleavage of DNA by topoisomerase II$\beta$-derived proteins. (a) Cleavage of the linear DNA substrate by 600 ng of each protein was assayed in the presence of 10 mM $Mg^{2+}$ (lanes 2, 8, 14, and 18), 10 mM $Mg^{2+}$ and 10 $\mu$g/mL m-AMSA (lanes 3, 9, 15, and 19), 10 mM $Ca^{2+}$ (lanes 4, 6, 10, 12, 16, and 20), or 10 mM $Ca^{2+}$ and 10 $\mu$g/mL m-AMSA (lanes 5, 7, 11, 13, 17, and 21). Topo II-cleaved DNA complexes were disrupted with SDS and proteinase K prior to precipitation with ethanol and electrophoresis on a 19% sequencing gel. Arrows indicate the 15- and 21-nucleotide cleavage products produced by cleavage of both labeled DNA strands. At this protein concentration, there is a linear relationship between protein concentration and the level of DNA cleavage. (b) Quantification of DNA cleavage by topo II$\beta$ and its mutants. Cleavage products were quantified as a percentage of wt cleavage in the presence of $Mg^{2+}$ and m-AMSA. Means and standard deviations ($SD^{n-1}$) were calculated from three experiments.

hydrolysis. Figure 5b shows that the dependence of ATP hydrolysis activity on magnesium concentration was similar for wt topo II$\beta$, $\beta$E477Q, and $\beta$K505E. These results suggest that coordination of the $Mg^{2+}$ ions involved in ATP binding and hydrolysis has not been significantly affected by either of these two mutations.

*DNA Cleavage Activity.* Cleavage of DNA by topoisomerase II requires the divalent cation $Mg^{2+}$ or $Ca^{2+}$. The cleavage−religation equilibrium of topo II on DNA can be studied by adding SDS to denature the protein and thus freeze the equilibrium. A 40 bp linear DNA substrate was used which contains a single topo II$\beta$ cleavage site which is cleaved strongly in the presence of *m*-AMSA, and weakly in its absence (*42*, *46*). In the presence of magnesium ions, the percentage of complexes in which the DNA is cleaved is very low (Figure 6a, lane 2); the level of cleavage is increased in the presence of topo II poisons, for example, *m*-AMSA (Figure 6a, lane 3). Calcium ions also increase the level of cleavage (Figure 6a, lane 4), and the level of cleavage is highest in the presence of both calcium and *m*-AMSA (Figure 6a, lane 5) (*14*, *45*, *47*).

The cleavage−religation equilibria of the topo II$\beta$ derivatives were analyzed in the presence of 10 mM $Mg^{2+}$ or $Ca^{2+}$, both with and without *m*-AMSA, to determine both their intrinsic cleavage levels and their responses to the drug. No cleavage was detected for $\beta$E447Q (Figure 6a, lanes 6 and 7) or $\beta$K505E (lanes 12 and 13) under any conditions. The level of cleavage by $\beta$R503E was reduced by more than 90% compared to that of wt topo II$\beta$, as none could not be detected in the presence of $Mg^{2+}$ or $Mg^{2+}$ with *m*-AMSA (Figure 6a, lanes 14 and 15), and only very weak cleavage was observed with $Ca^{2+}$ and $Ca^{2+}$ with *m*-AMSA (Figure 6a, lanes 16 and 17). Mutants $\beta$S480A and $\beta$R510Q both had 10−20% of wt topo II$\beta$ cleavage activity in the presence of $Mg^{2+}$ with *m*-AMSA (Figure 6a, lanes 9 and 19) or $Ca^{2+}$ (lanes 10 and 20). *m*-AMSA increased the level of $Ca^{2+}$-promoted cleavage by 5−6-fold for wt topo II$\beta$ and $\beta$S480A, and by 9−10-fold for $\beta$R510Q and $\beta$R503E (Figure 6b). Thus, it can be seen that all five mutations have significantly reduced the ability of topo II$\beta$ to cleave the 40 bp substrate. Furthermore, none of the mutants appear to have a reduced affinity for *m*-AMSA.

The decatenation studies presented above revealed that the optimal $Mg^{2+}$ concentration for decatenation was higher for $\beta$E477Q and $\beta$K505E (15−20 mM) than for wt topo II$\beta$ (5−10 mM). Cleavage assays were therefore carried out in the presence of a range of $Mg^{2+}$ and $Ca^{2+}$ concentrations (0−50 mM) for each topo II$\beta$ derivative. Figure 7 shows that wt topo II$\beta$ was very sensitive to $Mg^{2+}$ concentrations higher than 10 mM, but was tolerant of $Ca^{2+}$ up to 30 mM. The presence of *m*-AMSA reduced the sensitivity to $Ca^{2+}$ concentrations, with strong cleavage still observed at 50 mM. Mutants $\beta$S480A, $\beta$R503E, and $\beta$R510Q exhibited sensitivities to $Mg^{2+}$ and $Ca^{2+}$ similar to that of wt topo II$\beta$, both in the presence and in the absence of *m*-AMSA (data not shown). However, cleavage by $\beta$E477Q and $\beta$K505E was not observed at any of the $Mg^{2+}$ or $Ca^{2+}$ concentrations that were tested, including the optimal concentration for strand passage, 17.5 mM (Figure 7b and data not shown). Increasing the *m*-AMSA concentration did not induce cleavage by $\beta$E477Q or $\beta$K505E at any of the divalent cation concentrations (data not shown). This assay was also performed in the presence of clerocidin, a drug that irreversibly stabilizes the cleaved DNA intermediate (*48*). Clerocidin stimulated cleavage by wt topo II$\beta$, but not by $\beta$E477Q or $\beta$K505E at any of the $Mg^{2+}$ or $Ca^{2+}$ concentrations that were tested (data not shown). The detection limit of the cleavage assay is approximately 0.5% of the wt topo II$\beta$ cleavage in the presence of $Mg^{2+}$ and *m*-AMSA, indicating that the level of cleavage by these two mutants must be at least 100−200-fold lower than that of wt topo II$\beta$.

It was possible that mutants $\beta$E477Q and $\beta$K505E did not cleave the oligonucleotide substrate due to a switch in cleavage site specificity or a reduction in the binding affinity for *m*-AMSA. To investigate these possibilities, cleavage reactions were carried out on supercoiled plasmid DNA in the presence 17.5 mM $Mg^{2+}$ and ATP at a range of concentrations of several topo II poisons. No cleavage by $\beta$E477E or $\beta$K505E was observed in the presence of *m*-AMSA (Figure 8a, lanes 6−13), mitoxantrone (Figure 8b, lanes 6−13), or etoposide or clerocidin (data not shown), whereas cleavage by wt topo II$\beta$ was observed in the presence of all four drugs (Figure 8a,b, lanes 2−5, and data not shown).

Taken together, these data demonstrate that mutations S480A, R503E, and R510Q reduced the intrinsic level of DNA cleavage to less than 20% of that exhibited by wt topo II$\beta$, without inhibiting the stimulation induced by *m*-AMSA. Furthermore, mutations E477Q and K505E reduced the level of cleavage by more than 100−200-fold, such that the cleavage products were no longer detectable. Consequently, it was not possible to determine for these two mutants whether the optimal magnesium ion concentration for DNA cleavage had been altered, or whether the affinities for various topo II poisons had been reduced.

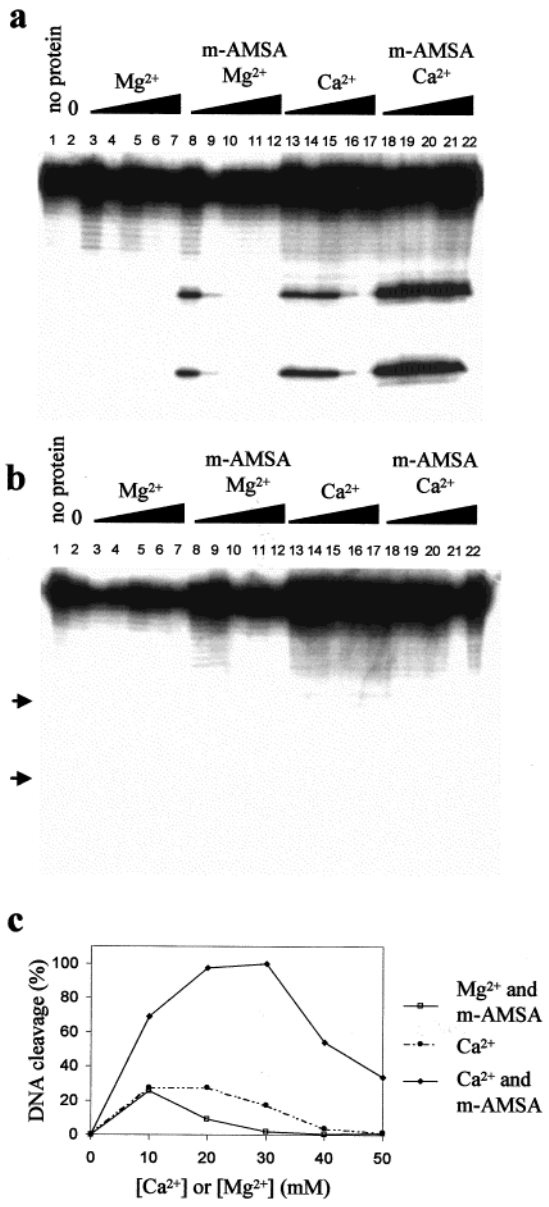


FIGURE 7: Dependence of the level of DNA cleavage on $Mg^{2+}$ concentration. Cleavage reactions were carried out with (a) 600 ng of wt topo II$\beta$ or (b) 600 ng of $\beta$K505E: lane 1, no protein; lanes 2−6, 10, 20, 30, 40, and 50 mM $Mg^{2+}$, respectively; lanes 7−11, 10, 20, 30, 40, and 50 mM $Mg^{2+}$, respectively, and 10 $\mu$g/mL m-AMSA; lanes 12−16, 10, 20, 30, 40, and 50 mM $Ca^{2+}$, respectively; and lanes 17−21, 10, 20, 30, 40, and 50 mM $Ca^{2+}$, respectively, and 10 $\mu$g/mL m-AMSA. (c) The level of cleavage by wt topo II$\beta$ in panel a is plotted against divalent cation concentration.

*DNA Binding Activity*. To determine whether the observed reductions in strand passage and DNA cleavage activities were the result of reduced DNA binding activity, the abilities of the topo II$\beta$ mutants to bind linear DNA were assayed using a gel retardation assay (Figure 9a) (*42*). The DNA substrate was the 40 bp duplex used for the cleavage assays described above, and the affinity of topo II$\beta$ for this substrate is 130 nM ($SD^{n-1} = 60$ nM) (*42*). Divalent cations are not required for DNA binding by topo II$\beta$ in this assay (*42*). All the mutants bound the linear DNA with efficiencies similar to that of the wild-type protein, as shown in panels a and c of Figure 9. Gel retardation assays were also carried out using four-way junction DNA as the substrate. Wt topo

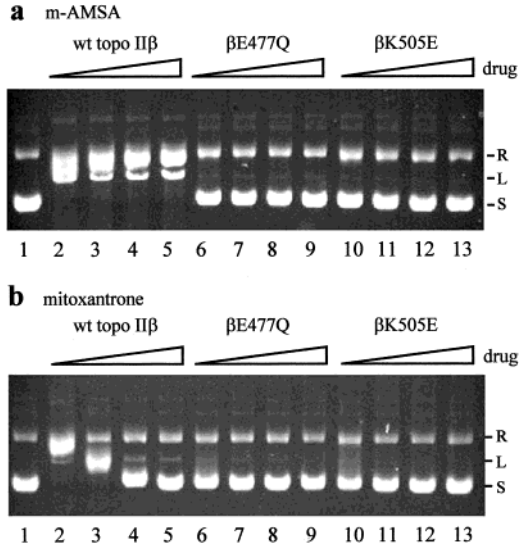


FIGURE 8: Drug-stimulated cleavage of plasmid DNA by wt topo II$\beta$, $\beta$E477Q, and $\beta$K505E. Wt topo II$\beta$, $\beta$E477Q, or $\beta$K505E (900 ng) was incubated with 1 $\mu$g of supercoiled plasmid DNA in relaxation buffer with 2 mM ATP and 17.5 mM $MgCl_2$ for 30 min at 37 °C in the presence of m-AMSA (a) or mitoxantrone (b). (a) m-AMSA was present at 10 $\mu$M (lanes 2, 6, and 10), 25 $\mu$M (lanes 3, 7, and 12), 50 $\mu$M (lanes 4, 8, and 12), or 100 $\mu$M (lanes 5, 9, and 13). (b) Mitoxantrone was present at 1 $\mu$M (lanes 2, 6, and 10), 2.5 $\mu$M (lanes 3, 7, and 11), 5 $\mu$M (lanes 4, 8, and 12), or 10 $\mu$M (lanes 5, 9, and 13). Cleavage reactions were stopped by adding SDS to a final concentration of 1% and proteinase K to a final concentration of 1 $\mu$g/mL, and then samples were incubated at 50 °C for 30 min. Samples were electrophoresed on a 0.8% agarose gel in TBE. Relaxed, linear (i.e., cleaved), and supercoiled DNA are indicated by R, L, and S, respectively.

II$\beta$ binds the four-way junction DNA 4-fold more strongly than the 40 bp linear DNA substrate (*42*). Binding titrations showed that wt topo II$\beta$ and the mutant proteins all had similar DNA binding profiles (Figure 9b and data not shown). The percentage of DNA complexed in the presence of 80 ng of each protein is shown in Figure 9c, and it can be seen that wt topo II$\beta$ and the five mutants all bound the four-way junction with comparable efficiencies. Furthermore, the efficiency of four-way junction binding by each protein was not altered when binding reactions were carried out at 37 °C, or when magnesium or calcium ions were present at a concentration of 10 mM (data not shown). These data show that none of the mutations have significantly altered the ability of topo II$\beta$ to bind either linear or four-way junction DNA.

## DISCUSSION

Seven separate mutations were created in the **E**GD**S**A, PL-(**R**/K)G**K**(I/M/L)LNV**R**, and IMT**D**(Q/A)DX**D** motifs of the B′ domain of human topo II$\beta$ (indicated in bold), and five of these mutants were studied systematically in vitro. Strikingly, mutants $\beta$E477Q and $\beta$K505E required an increased magnesium ion concentration for strand passage activity, with the apparent $K_M$ for $Mg^{2+}$ increasing from 2.7 mM in wt topo II$\beta$ to 9.7 mM in both mutants. Topo II requires $Mg^{2+}$ ions for two stages in the catalytic cycle, ATP hydrolysis and DNA cleavage (*45*). The data presented here indicate that binding of the magnesium ions for ATP hydrolysis was unaffected in mutants $\beta$E477Q and $\beta$K505E, whereas cleavage activity by these two mutants was unde-

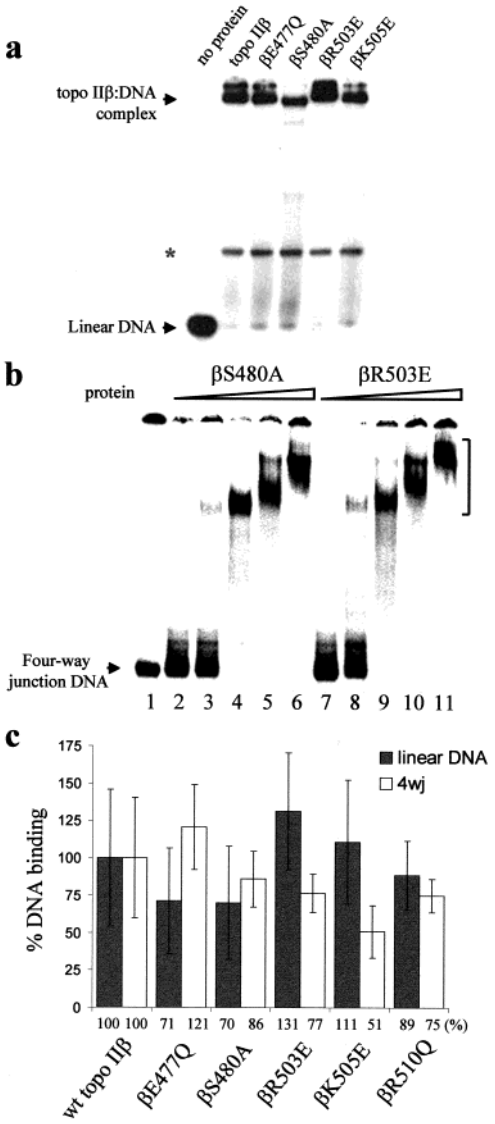


FIGURE 9: Gel retardation assay for comparing DNA binding by wt and mutant topoisomerase II$\beta$ derivatives. (a) Binding reaction mixtures contained the linear DNA substrate and 500 ng of wt topo II$\beta$, $\beta$E477Q, $\beta$S480A, $\beta$R503E, or $\beta$K505E as indicated above each lane. At this protein concentration, there is a linear relationship between the extent of complex formation and protein concentration. Reaction mixtures were incubated on ice for 45 min prior to electrophoresis at 4 °C on a native gel. The complex denoted by the asterisk is comprised of a contaminating DNA binding protein in the protein preparations. (b) Binding reactions were carried out as described for panel a, and the mixtures contained four-way junction DNA and $\beta$S480A (lanes 2−6) or $\beta$R503E (lanes 7−11): lane 1, no added protein; lanes 2 and 7, 25 ng of protein; lanes 3 and 8, 50 ng of protein; lanes 4 and 9, 100 ng of protein; lanes 5 and 10, 200 ng of protein; and lanes 6 and 11, 400 ng of protein. The topo II−DNA complexes are indicated by a bracket. (c) Bar chart of binding to the linear (gray bars) and four-way junction (white bars) DNA substrates by wt topo II$\beta$ and the mutants. To compare binding on the linear substrate, the protein−DNA complexes used in panel a and similar gels were quantified as a percentage of the total input DNA, and means and standard deviations ($SD^{n-1}$) were calculated from seven experiments. These are expressed as a percentage of the mean for wt topo II$\beta$. To compare binding on the four-way junction substrate, the percentage of bound DNA was plotted against protein concentration, and then the percentage of DNA which would be bound by 80 ng of protein was calculated by interpolation. This calculation was carried out separately for six experiments, and then means and standard deviations were calculated. The mean for wt topo II$\beta$ was set to 100%.

tectable. It is likely, therefore, that the increase in the optimal $Mg^{2+}$ concentration for strand passage is related to a reduction in the binding affinity for the $Mg^{2+}$ ion(s) required for DNA cleavage. These results indicate this area of the B′ domain may participate in $Mg^{2+}$ ion coordination and in DNA cleavage.

In contrast to $\beta$E477Q and $\beta$K505E, mutants $\beta$S480A, $\beta$R503E, and $\beta$R510Q did not alter the magnesium ion dependence of strand passage or DNA cleavage. However, these mutations all specifically reduced the level of DNA cleavage by at least 5-fold, indicating that the EGDSA and PL(R/K)GK(I/M/L)LNVR motifs play a role in promoting DNA cleavage that is distinct from that of $Mg^{2+}$ coordination. The reductions in the levels of DNA cleavage are paralleled by reductions of 25−65% in strand passage activity, which in turn are reflected in the abilities of the mutants to complement *ts* yeast topo II in vivo. It is possible that complementation ability has been affected by factors other than strand passage activity, however, for example, in vivo stability, or interactions with other cellular factors. These results parallel those of a recent study on yeast topo II, where the mutations E449A (**E**GDSA), N480A (PLRGKIL**N**), and D530A (IMTDQDH**D**) significantly reduced or abolished etoposide-stimulated DNA cleavage (*49*). Indeed, it is likely that the results presented here can be applied to all eukaryotic type II topoisomerases, not just topo II$\beta$, given the high degree of sequence conservation between these enzymes. It can be concluded that this conserved region of the B′ domain plays an important and specific role in the DNA cleavage−religation reaction.

*Relation to the Crystal Structure of S. cerevisiae Topo II.* All seven mutations are located in the B′ domain of wt topo II$\beta$, which is 57% identical to the equivalent region of yeast topo II. For clarity, the amino acid numbering of wt topo II$\beta$ will be used in the following discussion of the B′ domain. The computer program Modeller was used to model the amino acid sequence of the B′ domain of wt topo II$\beta$ onto the T2O crystal structure of yeast topo II (*5*), based on the alignment of Caron and Wang (*31*) (Figure 1B). The modeled topo II$\beta$ structure is very similar to that of yeast topo II, and the region containing the EGDSA, PLRGK(I/M)LNVR, and IMTDQD(Q/H)DGSH sequences is essentially the same in the two structures (Figure 1B). The three motifs are close to each other, and it is calculated that there is hydrogen bonding between them, as shown in Figure 10a.

Residues IMTDQD(Q/H)DGSH (554−564) form a loop, the base of which (indicated by underlined residues) is stabilized by hydrogen bonding from the EGDSA and PLRGK(I/M)LNVR sequences (shown diagramatically in Figure 10a). In particular, in both yeast topo II and human topo II$\beta$, the carboxyl group of E477 (**E**GDSA) forms a hydrogen bond with the hydroxyl group of T556, and the amino group of K505 [PLRG**K**(I/M)LNVR] forms a hydrogen bond with the backbone of D557. In contrast, the functional groups of residues S480, R503, and R510 do not participate in hydrogen bonding within the 92 kDa fragment, but instead are directed outward from the B′ domain. The similarities between the two structures suggest that the roles of E477 and K505 are conserved between wt topo II$\beta$ and yeast topo II. The data from in vitro experiments indicate that E477 and K505 may be involved in magnesium ion coordination. However, it seems unlikely that either E477

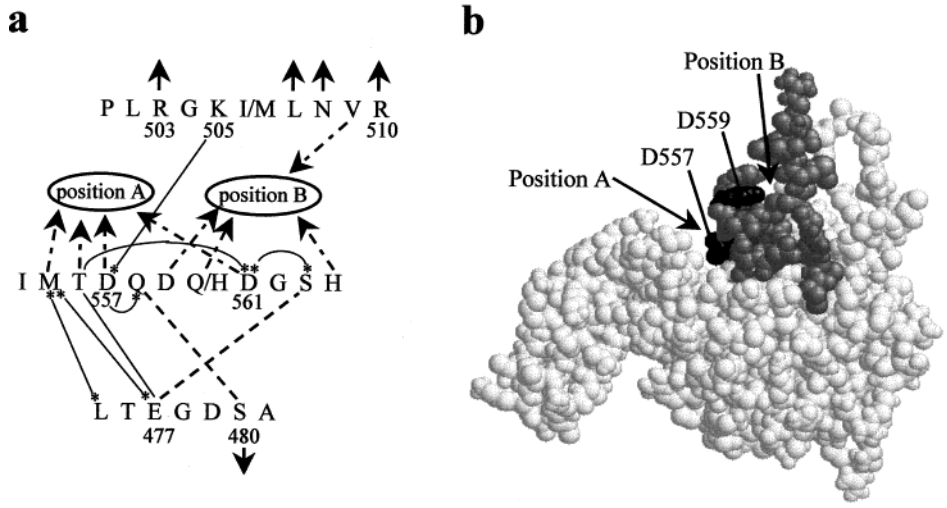


FIGURE 10: Two possible positions for the $Mg^{2+}$ binding site (positions A and B), as suggested by mutagenesis of the B′ domain of topo II$\beta$. (a) Schematic representation of the arrangement of the LTEGDSA, PLRGK(I/M)LNVR, and IMTDQD(Q/H)DGSH sequences in the B′ domain. Residues whose side chains point toward either one of the two proposed magnesium ion binding sites (positions A and B) are indicated by dotted arrows. Hydrogen bonds which are predicted to occur in both *S. cerevisiae* topo II and human topo II$\beta$ are represented by solid lines, and those that are only present in yeast topo II are represented by dotted lines (*5*). Hydrogen bonds to or from the peptide backbone are indicated by asterisks. Residues whose side chains point out of the B′ domain are represented by continuous arrows. (b) Space filling representation of the B′ domain of one *S. cerevisiae* topo II monomer. The EGDSA, PL(R/K)GK(I/L/M)LNVR, and IMTD-(Q/A)DXD motifs are shown in dark gray, and the residues corresponding to D557 and D559 in human topo II$\beta$ are shown in black.

or K505 could coordinate to $Mg^{2+}$ itself, either directly or via water molecules, as their functional groups participate in hydrogen bonding. It is more probable that they help to position other residues in the correct orientations for this role, in particular, those of the IMTDQD(Q/H)DGSH loop.

The three aspartate residues in the IMTDQD(Q/H)DGSH loop (D557, D559, and D561) are conserved in all type II topoisomerases, and are also conserved in topoisomerase IA enzymes (*29*, *31*). Comparisons of *E. coli* topo I with DNA polymerases have revealed that these acidic residues may participate in magnesium ion coordination (*30*, *32*). Topo II$\beta$ residues D557 and D561 [IMT**D**QD(Q/H)**D**GSH] were both mutated to N in this study, but the overproduced proteins were unstable and rapidly became degraded. It is interesting that these aspartate residues in yeast topo II both point into a solvent accessible space between the two $\alpha/\beta$ subdomains of the B′ domain (designated "position A" in panels a and b of Figure 10), as do adjacent residues M555 and T556 [I**MT**DQD(Q/H)DGSH]. Residue D561 does not form hydrogen bonds with any other residue, and in the yeast topo II structure, D557 only forms one hydrogen bond, which is with the peptide backbone of the adjacent residue, Q558. It is possible that position A is the location of a $Mg^{2+}$ binding site; it is solvent accessible and surrounded by several polar or charged residues, and disruption of hydrogen bonding to these surrounding residues increases the optimum $Mg^{2+}$ concentration for activity. However, residue D559 [IMT-DQ**D**(Q/H)DGSH] points into a second solvent accessible space, designated "position B" in panels a and b of Figure 10, which is on the opposite side of the IMTDQD(Q/H)-DGSH loop from position A. Position B is an alternative site for $Mg^{2+}$ binding, and the highly conserved H564 and the less well conserved Q560 (H in yeast topo II) are also directed into it. Mutation of E477 or K505 could destabilize the whole IMTDQD(Q/H)DGSH loop, thus reducing the affinity for $Mg^{2+}$ in either position A or B. Further mutagenic studies would help to further define the location of the $Mg^{2+}$ ion binding site. A recent report has shown that mutation of the residue equivalent to D561 in yeast topo II, D530A, yielded an enzyme with undetectable strand passage activity, and a low level of DNA cleavage activity (*49*). No studies on the $Mg^{2+}$ dependence of this mutant have been reported, however.

In the first structure of the yeast topo II fragment, subsequently termed T2O, the three conserved motifs of the B′ domain, EGDSA, PLRGK(I/M)LNVR, and IMTDQD-(Q/H)D, and in particular the two putative magnesium ion binding sites are all well removed from the catalytic active site (Figure 1) (*5*). However, comparative analysis of the crystal structures of *E. coli* topo I, DNA gyrase, and yeast topo II led Berger and co-workers to propose an alternate orientation for the B′ domain (*29*). In this model, the B′ domain is rotated with respect to the rest of the protein, such that the cluster of conserved acidic residues is placed in the neighborhood of the active site tyrosine. The B′ domain thus has the same orientation relative to the active site as the structurally similar domain 1 of *E. coli* topo I (*30*). This has recently been supported by a new crystal structure of yeast topo II, termed T2M, in which the B′ domains are rotated by 170° (*21*). Furthermore, this model is consistent with the recent demonstration that the active site tyrosine of one monomer cooperates with residues in the B′ domain of the second monomer to carry out DNA cleavage (*49*). In this scenario, a magnesium ion coordinated by the conserved aspartate residues of the B′ domain would be in a suitable position to help catalyze DNA cleavage. The biochemical data presented here provide support for the hypothesis that the conserved aspartate residues of the B′ domain participate in coordinating the magnesium ions(s) required for DNA cleavage.

In summary, mutagenic analysis of three conserved motifs in the B′ domain of topo II$\beta$ has revealed that this region is critical for DNA cleavage activity. Furthermore, mutations E477Q and K505E increase the optimal magnesium ion concentration for DNA strand passage activity. This is likely to result from a reduction in the binding affinity for the

magnesium ion(s) required for DNA cleavage. Examination of the crystal structure of yeast topo II reveals that residues E477 and K505 may assist in positioning three highly conserved aspartate residues, and we present a model in which these aspartate residues participate in magnesium ion coordination at two possible locations. When a recent model for the orientation of the B′ domain prior to DNA cleavage is taken into account (*29*), these motifs could participate in the arrangement of the active site, and in particular, one or more magnesium ions bound by the conserved aspartate residues would be in a prime position to help catalyze the DNA cleavage−religation reaction.

## ACKNOWLEDGMENT

We thank Adam West and Julio Herrera for critically reviewing this paper and Elaine Willmore for assistance in the preparation of the manuscript.

## REFERENCES

1. DiNardo, S., Voelkel, K., and Sternglanz, R. (1984) *Proc. Natl. Acad. Sci. U.S.A. 81*, 2616−2620.
2. Holm, C., Goto, T., Wang, J. C., and Botstein, D. (1985) *Cell 41*, 553−563.
3. Uemura, T., Ohkura, H., Adachi, Y., Morino, K., Shiozaki, K., and Yanagida, M. (1987) *Cell 50*, 917−925.
4. Wang, J. C. (1996) *Annu. Rev. Biochem. 65*, 635−692.
5. Berger, J. M., Gamblin, S. J., Harrison, S. C., and Wang, J. C. (1996) *Nature 379*, 225−232.
6. Sander, M., and Hsieh, T. (1983) *J. Biol. Chem. 258*, 8421−8428.
7. Liu, L. F., Rowe, T. C., Yang, L., Tewey, K. M., and Chen, G. L. (1983) *J. Biol. Chem. 258*, 15365−15370.
8. Worland, S. T., and Wang, J. C. (1989) *J. Biol. Chem. 264*, 4412−4416.
9. Harkins, T. T., and Lindsley, J. E. (1998) *Biochemistry 37*, 7292−7298.
10. Harkins, T. T., Lewis, T. J., and Lindsley, J. E. (1998) *Biochemistry 37*, 7299−7312.
11. Lindsley, J. E., and Wang, J. C. (1991) *Proc. Natl. Acad. Sci U.S.A. 88*, 10485−10489.
12. Roca, J., and Wang, J. C. (1992) *Cell 71*, 833−840.
13. Sugino, A., Higgins, N. P., Brown, P. O., Peebles, C. L., and Cozzarelli, N. R. (1978) *Proc. Natl. Acad. Sci U.S.A. 75*, 4838−4842.
14. Osheroff, N., Shelton, E. R., and Brutlag, D. L. (1983) *J. Biol. Chem. 258*, 9536−9543.
15. Chen, A. Y., and Liu, L. F. (1994) *Annu. Rev. Pharmacol. Toxicol. 34*, 191−218.
16. Reece, R. J., and Maxwell, A. (1989) *J. Biol. Chem. 264*, 19648−19653.
17. Brown, P. O., Peebles, C. L., and Cozzarelli, N. R. (1979) *Proc. Natl. Acad. Sci. U.S.A. 76*, 6110−6119.
18. Gellert, M., Fisher, L. M., and O'Dea, M. H. (1979) *Proc. Natl. Acad. Sci. U.S.A. 76*, 6289−6293.
19. Austin, C. A., Marsh, K. L., Wasserman, R. A., Willmore, E., Sayer, P. J., Wang, J. C., and Fisher, L. M. (1995) *J. Biol. Chem. 270*, 15739−15746.
20. Cabral, J. H., Jackson, A. P., Smith, C. V., Shikotra, N., Maxwell, A., and Liddington, R. C. (1997) *Nature 388*, 903−906.
21. Fass, D., Bogden, C. E., and Berger J. M. (1999) *Nat. Struct. Biol. 6*, 322−326.
22. Wigley, D. B., Davies, G. J., Dodson, E. J., Maxwell, A., and Dodson, G. (1991) *Nature 351*, 624−629.
23. Tingey, A. P., and Maxwell, A. (1996) *Nucleic Acids Res. 24*, 4868−4873.
24. Yamagishi, J., Yoshida, H., Yamayoshi, M., and Nakamura, S. (1986) *Mol. Gen. Genet. 204*, 367−373.
25. Yoshida, H., Bogaki, M., Nakamura, M., Yamanaka, L. M., and Nakamura, S. (1991) *Antimicrob. Agents Chemother. 35*, 1647−1650.
26. Lee, M. S., Wang, J. C., and Beran, M. (1992) *J. Mol. Biol. 223*, 837−843.
27. Wasserman, R. A., and Wang, J. C. (1994) *Cancer Res. 54*, 1795−1800.
28. Wasserman, R. A., and Wang, J. C. (1994) *J. Biol. Chem. 269*, 20943−20951.
29. Berger, J. M., Fass, D., Wang, J. C., and Harrison, S. C. (1998) *Proc. Natl. Acad. Sci. U.S.A. 95*, 7876−7881.
30. Lima, C. D., Wang, J. C., and Mondragon, A. (1994) *Nature 367*, 138−146.
31. Caron, P. R., and Wang, J. C. (1993) in *Molecular Biology of DNA topoisomerases* (Andoh, T., Ikeda, H., and Oguro, M., Eds.) pp 243−263, CRC Press, Boca Raton, FL.
32. Beese, L. S., and Steitz, T. A. (1991) *EMBO J. 10*, 25−33.
33. Pritchard, A. E., and McHenry, C. S. (1999) *J. Mol. Biol. 285*, 1067−1080.
34. Wang, J., Yu, P., Lin, T. C., Konigsberg, W. H., and Steitz, T. A. (1996) *Biochemistry 35*, 8110−8119.
35. Davis, P. A., and Woody, R. W. (1996) *Biochemistry 35*, 144−152.
36. Sawaya, M. R., Pelletier, H., Kumar, A., Wilson, S. H., and Kraut, J. (1994) *Science 264*, 1930−1935.
37. Derbyshire, V., Grindley, N. D., and Joyce, C. M. (1991) *EMBO J. 10*, 17−24.
38. Austin, C. A., and Marsh, K. L. (1998) *BioEssays 20*, 215−226.
39. Meczes, E. L., Marsh, K. L., Fisher, L. M., Rogers, M. P., and Austin, C. A. (1997) *Cancer Chemother. Pharmacol. 39*, 367−375.
40. Lindsley, J. E., and Wang, J. C. (1993) *J. Biol. Chem. 268*, 8096−8104.
41. Nitiss, J., and Wang, J. C. (1988) *Proc. Natl. Acad. Sci. U.S.A. 85*, 7501−7505.
42. West, K. L., and Austin, C. A. (1999) *Nucleic Acids Res. 27*, 984−992.
43. Alazard, R., Ebel, C., Venien-Bryan, V., Mourey, L., Samama, J. P., and Chandler, M. (1998) *Eur. J. Biochem. 252*, 408−415.
44. Chan, V. T. W., Ng, S. W., Eder, J. P., and Schnipper, L. E. (1993) *J. Biol. Chem. 268*, 2160−2165.
45. Osheroff, N. (1987) *Biochemistry 26*, 6402−6406.
46. Marsh, K. L., Willmore, E., Tinelli, S., Cornarotti, M., Meczes, E. L., Capranico, G., Fisher, L. M., and Austin, C. A. (1996) *Biochem. Pharmacol. 52*, 1675−1685.
47. Osheroff, N., and Zechiedrich, E. L. (1987) *Biochemistry 26*, 4303−4309.
48. Kawada, S., Yamashita, Y., Fujii, N., and Nakano, H. (1991) *Cancer Res. 51*, 2922−2925.
49. Liu, Q., and Wang, J. C. (1999) *Proc. Natl. Acad. Sci. U.S.A. 96*, 881−886.

BI991328B